

The kinetic, thermodynamic, and adsorption isotherm analyses of the corrosion inhibition of synthetic extracellular polymeric substances

Liew Chien Go¹, Dilip Depan¹, William Holmes², August Gallo³, Kathleen Knierim³, Tre Bertrand⁴, Rafael Hernandez^{Corresp. 1, 2}

¹ Department of Chemical Engineering, University of Louisiana at Lafayette, Lafayette, Louisiana, United States

² Energy Institute of Louisiana, University of Louisiana at Lafayette, Lafayette, Louisiana, United States

³ Department of Chemistry, University of Louisiana at Lafayette, Lafayette, Louisiana, United States

⁴ Coastal Chemical Co. LLC, Broussard, Louisiana, United States

Corresponding Author: Rafael Hernandez

Email address: rafael.hernandez@louisiana.edu

Background. Extracellular polymeric substances (EPS) extracted from waste activated sludge (WAS) have previously shown its potential in corrosion inhibition. The aim of this study is to design a synthetic EPS formulation as a surrogate of natural WAS EPS to overcome the corrosion inhibition inconsistency in WAS EPS. The adsorption behavior of the designed inhibitor was studied by kinetic, thermodynamic, and adsorption isotherm analyses.

Methods. Synthetic EPS was formulated based on the typical chemical compositions of natural WAS EPS, i.e. proteins, carbohydrates, humic substances, nucleic acids, and uronic acids. It is a mixture of glutamic acid, carboxymethylcellulose, humic acid, thymine, and alginic acid. Its corrosion inhibition performance was tested with carbon steel in 3.64% NaCl saturated with CO₂, using the potentiodynamic polarization scanning technique. The corrosion kinetic parameters were evaluated using Arrhenius relationships while the thermodynamic adsorption parameters were examined using the Langmuir isotherm and Van't Hoff plot.

Results. The inhibition efficiency improved with increasing inhibitor concentration and temperature. The optimum performance was 94% with 204 mg/L of inhibitor applied at 70°C. The inhibition performance was controlled by both the concentration of inhibitor and temperature. Chemisorption of the inhibitor molecules contributed to the overall inhibition performance by adhering to Langmuir isotherm, deducing that the synthetic EPS formed a monolayer of protection film on the metal surface, reducing the contact of metal with the corrosive environment, thus, slowing down the overall corrosion rate.

1 **The kinetic, thermodynamic, and adsorption isotherm**
2 **analyses of the corrosion inhibition of synthetic**
3 **extracellular polymeric substances**

4

5 Liew Chien Go¹, Dilip Depan¹, William Holmes², August Gallo³, Kathleen Knierim³, Tre
6 Bertrand⁴, Rafael Hernandez^{1,2}

7

8 ¹ Chemical Engineering, University of Louisiana at Lafayette, Lafayette, LA, USA

9 ² Energy Institute of Louisiana, University of Louisiana at Lafayette, Lafayette, LA, USA

10 ³ Chemistry, University of Louisiana at Lafayette, Lafayette, LA, USA

11 ⁴ Coastal Chemical Co., LLC, Broussard, LA, USA

12

13 Corresponding Author:

14 Rafael Hernandez^{1,2}

15 131 Rex Street, Lafayette, LA, 70503, USA

16 Email address: rafael.hernandez@louisiana.edu

17 Abstract

18 **Background.** Extracellular polymeric substances (EPS) extracted from waste activated sludge
19 (WAS) have previously shown its potential in corrosion inhibition. The aim of this study is to
20 design a synthetic EPS formulation as a surrogate of natural WAS EPS to overcome the
21 corrosion inhibition inconsistency in WAS EPS. The adsorption behavior of the designed
22 inhibitor was studied by kinetic, thermodynamic, and adsorption isotherm analyses.

23

24 **Methods.** Synthetic EPS was formulated based on the typical chemical compositions of natural
25 WAS EPS, i.e. proteins, carbohydrates, humic substances, nucleic acids, and uronic acids. It is a
26 mixture of glutamic acid, carboxymethylcellulose, humic acid, thymine, and alginic acid. Its
27 corrosion inhibition performance was tested with carbon steel in 3.64% NaCl saturated with
28 CO₂, using the potentiodynamic polarization scanning technique. The corrosion kinetic
29 parameters were evaluated using Arrhenius relationships while the thermodynamic adsorption
30 parameters were examined using the Langmuir isotherm and Van't Hoff plot.

31

32 **Results.** The inhibition efficiency improved with increasing inhibitor concentration and
33 temperature. The optimum performance was 94% with 204 mg/L of inhibitor applied at 70°C
34 (343 K). The inhibition performance was controlled by both the concentration of inhibitor and
35 temperature. Chemisorption of the inhibitor molecules contributed to the overall inhibition
36 performance by adhering to Langmuir isotherm, deducing that the synthetic EPS formed a
37 monolayer of protection film on the metal surface, reducing the contact of metal with the
38 corrosive environment, thus, slowing down the overall corrosion rate.

39

40 Introduction

41 Extracellular polymeric substances (EPS) are the metabolic products produced by most
42 microorganisms. They accumulate on the surface of microorganisms, acting as protective
43 barriers against the microorganisms' external environment [1]. Typically, carbohydrates have
44 been identified as the major constituents in the EPS of many pure cultures [2][3], whereas
45 proteins were found in substantial quantities in the sludge of many wastewater treatment reactors
46 [1][4]. Small amounts of humic substances [5], uronic acids, and nucleic acids [1][6][7] were
47 also detected in EPS. A previous study [8][9] showed the potential of EPS extracted from waste
48 activated sludge (WAS) of wastewater treatment operations as a green corrosion inhibitor for
49 CO₂ corrosion. A maximum inhibition performance of about 80% was achieved with the
50 application of 1000 mg/L of this inhibitor. The corrosion inhibition mechanism of WAS EPS
51 was explained by the formation of a biofilm on the metal surface, shielding the metal surface
52 from the corrosive environment. Even though the inhibition performance is comparable to
53 commercial products, the nature of WAS caused inconsistency in inhibition efficiency. The
54 composition of WAS is dependent on wastewater treatment operational parameters, such as inlet
55 biochemical oxygen demand and sludge residence time.

56 This study focused on the evaluation of a corrosion inhibitor from the surrogate of WAS
57 EPS. The reason of making the surrogate was to have control on the chemical composition of the
58 corrosion inhibitor used and ensure consistent inhibition performance. This study hypothesized

59 that the designed synthetic EPS will demonstrate similar corrosion inhibition behavior as the
60 natural WAS EPS because it was formulated based on the major chemical compositions of
61 natural WAS EPS. The novelty of this research was the design of a surrogate biomass-based
62 corrosion inhibitor inspired by sources with varied chemical compositions. To the knowledge of
63 the authors, this line of work has not been reported elsewhere. This study is unique in the way
64 that it is a multidisciplinary work. Bio-inspired systems and materials are not uncommon in the
65 literature. Yet, this concept is the pioneer of the field of corrosion inhibitor formulation
66 development. For instance, some of the most commonly applied programming algorithms in
67 computer science and engineering today are bio-inspired. Algorithms like genetic and ant colony
68 mimic the natural biological systems to solve research problems. This study is adopting the bio-
69 inspired concept into the corrosion inhibitor formulation development. It is believed that this line
70 of multidisciplinary work could benefit and advance the research in corrosion inhibitor
71 development, especially the renewable type.

72 The present study seeks to investigate the corrosion inhibitive properties of synthetic EPS
73 for carbon steel in 3.64% NaCl solution saturated with CO₂ gas using the potentiodynamic
74 polarization technique. The corrosion kinetic parameters and thermodynamic adsorption
75 parameters are calculated and reported.

76

77 **Materials & Methods**

78 **Metal specimen preparation**

79 Potentiodynamic polarization scans were performed on carbon steels of the following
80 weight percentage composition: 0.17 C, 0.08 Mn, 0.014 P, 0.002 S, 0.022 Si, 0.02 Cu, 0.01 Ni,
81 0.04 Cr, 0.002 Sn, 0.042 Al, 0.006 N, 0.001 V, 0.0001 B, 0.001 Ti, 0.001 Cb, and the remainder
82 iron. The pre-treatment of the specimens' surface was carried out by grinding with sandpapers of
83 40, 220, 320 grits, rinsing with deionized water, then drying with paper towel. The specimens
84 were used immediately after pre-treatment.

85 **Corrosive medium preparation**

86 The corrosive medium was prepared with 36.4 g of NaCl (Fisher Scientific, Hampton,
87 NH, USA) in 1 L of deionized water to make up 3.64% of NaCl solution. The deionized water
88 used was drinking water filtered with Milli-Di Water Purification System (Merck Millipore,
89 Burlington, MA). Prior to starting of each experiment, CO₂ gas was sparged in the test solution
90 at 30 psi for 30 minutes. Then, the solution was transferred into the reactor, with CO₂ gas
91 continuously sparging throughout the experiment at 20 psi.

92 **Corrosion inhibitor preparation**

93 A mixture of several chemical compounds was labelled as synthetic EPS. It was used as
94 the test corrosion inhibitor in this study. The details of each compound, i.e. chemical type,
95 compound identity, vendor, specification, and composition, are listed in Table 1. These
96 compounds were mixed in the given composition as synthetic EPS. The concentrations of
97 inhibitors used in the following runs were doubled, tripled, and quadrupled.

98 **Potentiodynamic polarization method**

99 Potentiodynamic polarization experiments were carried out with Gamry Flexcell Critical

100 Pitting Cell Kit, connecting to the Gamry Potentiostat Interface 1000. The reference, counter,
101 and working electrodes used were saturated calomel electrode (SCE), graphite rod, and the metal
102 specimen, respectively. The setup was equipped with a heating jacket connected to TDC4
103 Omega temperature controller to maintain the test solution at a desired temperature, in this case,
104 25°C, 50°C, and 70°C. The Glas-Col GT Series stirrer was connected to the setup externally and
105 adjusted to 50 rpm to get the desired shear and to ensure even heating. The working solution
106 volume was 1 L. The working area of the metal specimens had a circular form of 5 cm².

107 The potentiodynamic polarization scans were carried out in potential range of -0.25 to
108 +0.25 V versus corrosion potential (E_{corr}) at a scan rate of 3 V/hr. Corrosive medium was added
109 into the reactor with carbon dioxide gas sparging constantly at 20 psi throughout the experiment.
110 The reactor was allowed to equalize for 30 minutes prior to the beginning of experiment. After
111 the system was equalized, Tafel plots were graphed with Gamry DC105 DC Corrosion
112 Technique Software until three relatively similar readings were obtained. Next, corrosion
113 inhibitor was added into the reactor. The reactor was again allowed to equalize for 30 minutes,
114 then Tafel plots were graphed. This step was repeated until three consecutive graphs with similar
115 trends were yielded, to ensure the stability of the system. Subsequently, the concentration of the
116 corrosion inhibitor was increased. Again, the system was being equalized for 30 minutes,
117 followed by the graphing of Tafel plots.

118 The Tafel plot was plotted with the mean values of corrosion potential (E_{corr}) and
119 corrosion current density (I_{corr}) from the triplicates of the experiments, while the electrochemical
120 parameters obtained from the curves were reported with mean and standard deviation. The
121 corrosion current densities were found by extrapolating the linear Tafel segment of the anodic
122 and cathodic curves to the corrosion potential. The corrosion inhibition efficiency was then
123 calculated with Equation 1.

$$124 \quad \text{Inhibition Efficiency (\%)} = \frac{I_{\text{corr, uninhibited}} - I_{\text{corr, inhibited}}}{I_{\text{corr, uninhibited}}} \times 100\% \quad (1)$$

125 Fourier-transform infrared spectroscopy (FTIR)

126 Agilent Cary 630 FTIR incorporated with MicroLab software were used for the FTIR
127 analysis in this study. This equipment worked based on Attenuated Total Reflection (ATR)
128 Method. The scanning was range between 4000 to 400 cm⁻¹ with resolution of 4 cm⁻¹.

129

130 Results

131 Corrosion inhibition performance

132 The Tafel plots generated from the potentiodynamic polarization measurements for
133 carbon steel in 3.64% NaCl saturated with CO₂ gas with synthetic EPS range from 51 mg/L to
134 204 mg/L at 25°C, 50°C, and 70°C (298 K, 323 K, 343 K) are presented in Figure 1, Figure 2,
135 and Figure 3, respectively. The details of electrochemical parameters obtained from the curves,
136 namely corrosion potential (E_{corr}), corrosion current density (I_{corr}), and inhibition efficiency, are
137 listed in Table 2. Moreover, the effects of inhibitor concentration and media temperature are
138 addressed in the discussion section. It is also worth noting that the significance of operation and
139 economics of the synthetic EPS as an oil field corrosion inhibitor formulation is also included in
140 the discussion section.

141 **Corrosion kinetic parameters**

142 Corrosion kinetic parameters, i.e. apparent activation corrosion energy (E_a), enthalpy of
143 activation (ΔH_a°), and entropy of activation (ΔS_a°), are listed in Table 3. Two Arrhenius plots
144 used for the evaluation of these corrosion kinetic parameters are shown in Figure 4 and Figure 5.
145 The details of calculations are discussed in the discussion section.

146 **Thermodynamic adsorption parameters**

147 The standard free energy of adsorption (ΔG_{ads}°), enthalpy of adsorption (ΔH_{ads}°), and the
148 entropy of adsorption (ΔS_{ads}°) are listed in Table 4. The Langmuir isotherm and the Van't Hoff
149 plots are shown in Figure 6 and Figure 7, respectively. The equations and graphs involved for the
150 thermodynamic adsorption parameters are explained in the discussion section.

151 **FTIR**

152 The IR spectra is shown in Figure 8 **Error! Reference source not found.** and the
153 characteristic IR absorption frequencies of the responding organic functional groups of synthetic
154 EPS is tabulated in Table 5.

155

156 **Discussion**

157 **Properties of synthetic EPS**

158 Synthetic EPS is a mixture of several major groups of chemicals in natural WAS EPS.
159 Although there are many ways to extract EPS and each of the methods give different chemical
160 composition [1][7][10]; the composition of synthetic EPS formulated in this study will be based
161 on the method of heating. Typically, the EPS extracted by heating has the highest proteins
162 concentration, followed by carbohydrates, humic substances, nucleic acids, and uronic acids
163 [1][7][10]. Therefore, proteins will be the basis of the synthetic EPS and the ratio of different
164 chemicals will be based on the proteins. The compounds were mixed in ratios that were realistic
165 (small enough concentration to be able to measure accurately using an analytical balance) to be
166 acted as a corrosion inhibitor. They were mixed according to the following ratios:

- 167 a. Proteins:carbohydrates = 2.5:1
- 168 b. Proteins:humic substances = 6:1
- 169 c. Proteins:nucleic acids = 15:1
- 170 d. Proteins:uronic acids =15:1

171 One compound was selected from each chemical group. They were chosen based on their
172 structures and their chemical inhibition performances in the literature. Structure wise,
173 compounds with nitrogen, oxygen, or sulfur atoms were preferred since all organic corrosion
174 inhibitors typically contain at least one of these atoms, almost without exception. In addition,
175 bigger compounds are also typically preferred as corrosion inhibitors because bigger compounds
176 are more effective in separating the metal surface from its corrosive environment when adsorbed
177 on the metal surface. The compounds chosen for the synthetic EPS mixture fulfilled these
178 descriptions, as illustrated in Figure 9. Furthermore, those chemicals that had demonstrated
179 corrosion inhibition were prioritized to be the candidates in the pool of selection. For protein, an
180 amino acid, which is the building block of a protein was chosen. Glutamic acid, a common

181 component of bacterial cell wall [11], made an excellent candidate as an amino acid for the
182 purpose of this study since it has also been proven to be an effective corrosion inhibitor in
183 several studies [12][13]. Glutamic acid showed approximately 54 to 90% of inhibition efficiency
184 in 0.5 M HCl with copper [12][13]. Due to its potential in corrosion inhibition, it was chosen as
185 the main component of the synthetic EPS. The second biggest composition was carbohydrate.
186 For an organic corrosion inhibitor, typically, a bigger molecule is preferred.
187 Carboxymethylcellulose (CMC), a relatively big molecular weight packed with multiple oxygen
188 atoms, was selected as the candidate for the chemical group of carbohydrate. Its corrosion
189 inhibition capability has also been proven excellent in various investigations [14][15]. Inhibition
190 efficiencies of about 65 to 72% were observed when CMC was used with mild steel in acid
191 solutions H₂SO₄ [14] and HCl [15], respectively. However, corrosion inhibition studies on the
192 rest of the chemical groups have no record in the literature to date. For humic substances and
193 uronic acids, there are not many chemicals from these groups, so, humic acid and alginic acid
194 were picked for each group, respectively. In the case of nucleic acids, there are only four choices
195 in this group, namely thymine, guanine, adenine, and cytosine. Making a decision based on an
196 economical point of view, the most affordable choice was thymine. Thymine is a relatively
197 smaller compound compared to other chosen chemicals, but it contains both nitrogen and oxygen
198 atoms, making it a desirable option. Hence, glutamic acid, CMC, humic acid, thymine, and
199 alginic acid were chosen as the formulation for synthetic EPS. Their chemical structures are
200 shown in Figure 9.

201 The potential of utilizing biomass sources directly as corrosion inhibitors are undeniable.
202 There is an enormous amount of studies on the application of plant extracts as corrosion
203 inhibitors, but these products are still relatively rare in the market. One of the main reasons that
204 is delaying the commercialization of these inhibitors could be the current immature resource
205 recovery techniques. A lot of extraction methods are still economical infeasible these days.
206 Therefore, in order to promote the use of renewable corrosion inhibitors, as well as to improve
207 the marketability of these products, a bio-inspired corrosion inhibitor formulation is introduced
208 in this study. Compared to the traditional plant extracts corrosion inhibitors, this type of
209 renewable corrosion inhibitor is more market-ready because of several advantages: (1) renewable
210 sources, (2) economic feasibility, (3) chemical composition consistency, as well as (4) corrosion
211 inhibition performance consistency.

212

213 **Effect of concentration**

214 The curves in Figure 1, Figure 2, and Figure 3 revealed well defined anodic and cathodic
215 polarization Tafel regions. Note that only one set of experimental data was reported because the
216 differences in triplicates were insignificant. The results for the triplicates can be found in the raw
217 data section.

218 As observed in these figures, both cathodic and anodic reactions of carbon steel electrode
219 corrosion were inhibited by the increase concentration of synthetic EPS in 3.64% NaCl saturated
220 with CO₂ gas. This observation indicates that the addition of synthetic EPS reduced anodic
221 dissolution as well as the hydrogen evolution reaction [16]. This can be explained by the
222 adsorption of inhibitor over the corroded surface [17]. Tafel lines of nearly equal slopes were
223 obtained, indicating that the hydrogen evolution reaction was activated-controlled [18].

224 The details of electrochemical parameters obtained from the Tafel plots such as the
225 values of corrosion potential, E_{corr} , corrosion current density, I_{corr} , corrosion protection
226 efficiency, and surface coverage degree, θ , are presented in Table 2. The corrosion inhibition
227 efficiency was calculated using Equation 1, based on the I_{corr} values, where $I_{\text{corr,blank}}$ and I_{corr} were
228 the corrosion current density without and with inhibitor, respectively. These values were
229 obtained by the extrapolation of the cathodic and anodic Tafel lines to the corrosion potentials.
230 The data showed that the I_{corr} values decreased in the presence of synthetic EPS. These values
231 also dropped as the concentration of inhibitor increased, meaning that the corrosion reaction was
232 slowing down as the inhibitor concentration was increasing. This phenomenon can be attributed
233 to the adsorption of synthetic EPS on the metal surface [18].

234 There was no definite pattern observed in E_{corr} values in the presence of different
235 concentrations of synthetic EPS. This result indicated that synthetic EPS may be considered as a
236 mixed-type corrosion inhibitor [19] in the presence of CO_2 gas saturated 3.64% NaCl solution.
237 The maximum displacement in E_{corr} of less than 0.085 V suggests a mixed mode of inhibition
238 [20]. Mixed-type corrosion inhibitor retards corrosion rate by suppressing both anodic and
239 cathodic corrosion reactions, typically by adsorbing on a metal surface, forming a protective film
240 to reduce contact of metal surface from the corrosive environment [21].

241 The inhibition efficiency increased as the concentration of synthetic EPS increased. The
242 maximum inhibition was about 94% with an optimum inhibitor concentration of 204 mg/L at
243 70°C. At 25°C, the maximum inhibition protection of synthetic EPS was 82% at a concentration
244 of 153 mg/L. The previous study of WAS EPS inhibitor demonstrated an optimum inhibition
245 performance of about 79% at a concentration of 1000 mg/L [8]. Even though the inhibition
246 performance showed only a mere improvement of 3%, the inhibitor concentration was reduced
247 by about 6.5 times. It is known that the natural WAS EPS is rich in a variety of compounds.
248 These compounds could have posed steric hindrance on the adsorption of inhibition molecules
249 on the metal surface, bring down the efficiency of the overall inhibition performance, so, higher
250 concentrations of inhibitors were required to demonstrate the corrosion inhibition capability.
251 Unlike the natural WAS EPS, the synthetic EPS was formulated specifically on the EPS groups
252 that are known to perform as corrosion inhibitors. Hence, it is expected that the corrosion
253 inhibition efficiency of synthetic EPS to be higher than the natural WAS EPS. Furthermore, in
254 the case of commercial corrosion inhibitors, their corrosion protection performances are typically
255 above 70%. Synthetic EPS has a corrosion inhibition performance that is within the range of
256 commercial corrosion inhibitors. One advantage compared to natural WAS EPS is that its
257 inhibition performance is consistent. The results obtained from this study strongly suggest the
258 great potential commercialization value of synthetic EPS as a valuable material to inhibit
259 corrosion issues in oilfield operations.

260

261 **Effect of temperature**

262 The effect of temperature on the inhibited solution–metal reaction is highly complex
263 because many changes could occur on the metal surface such as rapid etching and desorption of
264 inhibitor, also, the inhibitor itself may undergo decomposition and/or rearrangement [22]. The
265 effect of corrosion inhibition by synthetic EPS in NaCl solution saturated with CO_2 gas was
266 studied with three different temperatures, i.e. 25°C, 50°C, and 70°C. Since the corrosion rate is
267 greatly affected by the concentration of inhibitor as well as the temperature of the working

268 environment, these factors have an important operational impact.

269 At different temperatures and inhibitor concentrations, the corrosion inhibition
270 efficiencies varied. It was apparent that the rates of carbon steel corrosion, both in the blank
271 solution of 3.64% NaCl saturated with CO₂ gas and with the presence of corrosion inhibitor,
272 increased with increasing temperature. The impact of temperature on the overall corrosion
273 reaction was more pronounced than the effect of inhibitor concentration. The inhibition
274 efficiency increased with temperature. Typically, a decrease in inhibition efficiency with a rise in
275 temperature suggests physisorption of the corrosion inhibitor. In contrast, an increase in
276 inhibition efficiency with rise in temperature is indicative of a chemisorption mechanism [23].
277 Therefore, the results clearly indicate a chemisorption mechanism of synthetic EPS on the carbon
278 steel surface.

279 Corrosion kinetic parameters

280 Corrosion kinetics parameters can be evaluated with different approaches. This study
281 seeks to quantitatively evaluate the performance of the studied corrosion inhibitor (synthetic
282 EPS) using an engineering calculation approach that yields empirical results. Instead of focusing
283 mechanistically on the chemistry of the corrosion and corrosion inhibitor reactions to obtain the
284 corrosion kinetics parameters, it is looking at an engineering perspective that is tailored to the
285 studied system. The chemistry of the corrosion and corrosion inhibitor reactions are unutterably
286 important, but it is not the center of the study. This study is not set up to investigate the
287 mechanistic values of the corrosion kinetic and thermodynamic adsorption parameters.

288 This paper emphasizes on the engineering significance of the synthetic EPS as a corrosion
289 inhibitor by applying engineering equations that are based on basic corrosion theory but adapted
290 heuristically to the studied system. Since the reported numbers (i.e. apparent activation corrosion
291 energy, enthalpy of activation, entropy of activation) are empirical values that are only relevant
292 to the studied system, these numbers may not be duplicated with other system set up (e.g.
293 traditional weight loss method with beaker testing). Even though the reported numbers are not
294 the mechanistic values with respect to the theoretical corrosion reactions and the theoretical
295 adsorption of the inhibitors, it serves a purpose to screen the performance of the studied
296 corrosion inhibitor quantitatively using engineering calculations. In addition, the empirical
297 values are also helpful in determining the behavior of the inhibitor in the studied system. For
298 example, the enthalpy of activation could be used to describe whether the metal dissolution
299 process is endothermic or exothermic. The idea is that, by adhering to the same experimental set
300 up and procedure, the same engineering calculations can be performed to estimate the same
301 parameters for other inhibitors, serving as a comparison model. This is a particularly valuable
302 heuristic tool, where the corrosion inhibitor can be screened rapidly. Thus, if the results obtained
303 from the experiment are encouraging, further corrosion testing such as sparged beaker test and
304 wheel test could be considered. Furthermore, the same approach has previously been
305 demonstrated in the literature [24][25], proven its usability and reliability.

306 The activation parameters for the corrosion reaction were calculated using an Arrhenius-
307 type plot according to Equation 2. It is worth mentioning that the Arrhenius equations applied
308 were tailored to the studied system, as a heuristic approach to estimate the empirical values of
309 the apparent activation corrosion energy, enthalpy of activation, and entropy of activation that

310 are true to the system. E_a in the equation denotes the apparent activation corrosion energy, R is
 311 the universal gas constant, and k is the Arrhenius pre-exponential factor. The values of apparent
 312 activation energy of corrosion were determined from the slope of $\ln I_{corr}$ versus $1/T$ plot, shown
 313 in Figure 4. The data showed lower activation energy in the presence of inhibitors than in its
 314 absence, which is a typical pattern of chemisorption [18].

315 An alternative formulation of Arrhenius equation, i.e. transition-state equation shown in
 316 Equation 3, was used to calculate the change of enthalpy (ΔH_a°) and entropy (ΔS_a°) of activation
 317 for the activation complex formation in the transition state. In this equation, the h is the Planck's
 318 constant, N is the Avagadro's number, ΔS_a° is the entropy of activation, and ΔH_a° is the enthalpy
 319 of activation. Figure 5 shows a plot of $\ln(I_{corr}/T)$ against $1/T$ for synthetic EPS. A straight line
 320 was obtained with a slope of $\Delta H_a^\circ/R$ and an intercept of $\ln(R/Nh + \Delta S_a^\circ/R)$, from which the
 321 values of ΔH_a° and ΔS_a° were calculated. The positive enthalpy values reflected the endothermic
 322 nature of metal dissolution process. Large and negative values of entropy imply that the activated
 323 complex in the rate determining step represents an association rather than a dissociation step
 324 [18].

$$325 \quad I_{corr} = k e^{-\frac{E_a}{RT}} \quad (2)$$

$$326 \quad I_{corr} = \frac{RT}{Nh} \exp\left(\frac{\Delta S_a^\circ}{R}\right) \exp\left(-\frac{\Delta H_a^\circ}{RT}\right) \quad (3)$$

327 Thermodynamic adsorption parameters

328 Adsorption isotherms provide insights into the interaction among the adsorbed molecules
 329 and the metal surface, which can help to better understand the corrosion inhibition mechanism.
 330 The values of surface coverage (θ) to different concentrations of inhibitor, obtained from the
 331 polarization measurements in the temperature range of 25 to 70°C (298 to 343 K) were used to
 332 explain the best isotherm to determine the adsorption mechanism. The values of θ were assumed
 333 to be the corrosion inhibition efficiencies. The reason being, without the presence of inhibitor
 334 compound, an inhibition efficiency of 0% is expected, so, when an inhibitor compound is
 335 introduced to a corrosive environment, the improved corrosion inhibition efficiency is believed
 336 to be solely contributed by the coverage of the inhibitor compound on the metal surface. The
 337 surface coverage, θ , were used in a series of equations shown in Equation 4, Equation 5, and
 338 Equation 6 [26]. Equation 4 showed the relationship of I_{corr} , $I_{corr,blank}$, I_{sat} , and θ . I_{sat} is the current
 339 density of entirely covered surface. This equation was then be rearranged into Equation 5. As I_{corr}
 340 was greater than I_{sat} , Equation 5 was simplified to Equation 6.

$$341 \quad I_{corr} = (1 - \theta)I_{corr,blank} + \theta I_{sat} \quad (4)$$

$$342 \quad \theta = \frac{I_{corr,blank} - I_{corr}}{I_{corr,blank} - I_{sat}} \quad (5)$$

$$343 \quad \theta = \frac{I_{corr,blank} - I_{corr}}{I_{corr,blank}} \quad (6)$$

344 In the range of temperature and inhibitor concentration studied, the best correlation
 345 between the experimental results and the adsorption isotherm functions was obtained using
 346 Langmuir adsorption isotherm. The Langmuir isotherm for monolayer adsorption is given by
 347 Equation 7. By linearizing this equation, Equation 8 was obtained.

$$348 \quad \frac{\theta}{1-\theta} = KC \quad (7) \quad \frac{C}{\theta} = \frac{1}{K} + C$$

$$349 \quad (8)$$

350 In Equation 7 and Equation 8, θ is the surface coverage degree, C is the inhibitor
 351 concentration in the NaCl solution, and K is the equilibrium constant of the adsorption process.
 352 The correlation coefficient, R^2 , was used to describe how close the isotherm fits the experimental
 353 data. The plot of C/θ against C gave a straight line and the linear correlation coefficients were
 354 fairly close to 1, indicating good fit to the data. This graph is shown in Figure 6. The adsorption
 355 behavior of synthetic EPS conformed to Langmuir isotherm, suggesting monolayer adsorption,
 356 which is a typical behavior of chemisorption [27].

357 In general, Langmuir isotherm is not recommended to be used to describe a mixture
 358 system because the individual components in a mixture can each be adsorbed in different ways.
 359 However, it is applicable to this study because the synthetic EPS, as a corrosion inhibitor
 360 formulation, was treated as an entity. The individual contribution of compounds in the mixture of
 361 synthetic EPS were considered unimportant, therefore, being omitted. These are the basic
 362 assumptions of Langmuir isotherm: (1) surface of the adsorbent (metal) is uniform, (2)
 363 adsorption sites are equivalent, (3) adsorbed molecules do not interact, (4) all adsorption occurs
 364 through the same mechanism. Assuming that the metal surface is uniform, the adsorption sites
 365 are equivalent, and the inhibitor formulation is being treated as an entity, Langmuir isotherm is
 366 appropriate to be used to describe the overall adsorption mechanism. There are numerous studies
 367 in the literature where Langmuir was used to describe the adsorption mechanism of an inhibitor
 368 mixture, especially plant extracts [28][29].

369 K values were calculated from the intercepts of the same plot (Figure 6). The constant of
 370 adsorption, K , can be related to the standard free energy of adsorption, ΔG_{ads}° , using Equation 9.
 371 The constant 1×10^6 in the equation is the concentration of water molecules expressed in mg/L,
 372 R is the universal gas constant, T is the absolute temperature. On the other hand, ΔH_{ads}° can be
 373 deduced from the integrated version of the Van't Hoff equation expressed by Equation 10
 374 **Reference source not found.** Figure 7 shows the plot of $\ln K$ versus $1/T$ which yield a straight
 375 line with a slope of $-\Delta H_{ads}^\circ/R$. The value obtained was used to find the ΔH_{ads}° . The calculated
 376 ΔH_{ads}° was then used to calculate the values of ΔS_{ads}° by using Equation 11.

$$377 \quad \Delta G_{ads}^\circ = -RT \ln (1 \times 10^6 K) \quad (9)$$

$$378 \quad \ln K = -\frac{\Delta H_{ads}^\circ}{RT} + \frac{\Delta S_{ads}^\circ}{R} \quad (10)$$

$$379 \quad \Delta G_{ads}^\circ = \Delta H_{ads}^\circ - T\Delta S_{ads}^\circ \quad (11)$$

380 A more in-depth study of the inhibitor adsorption mechanism was investigated using the
 381 values of thermodynamic parameters. The details can be found in Table 4. The spontaneity of the
 382 adsorption of inhibitor on the metal surface as well as the stability of the adsorbed layer on the
 383 metal surface was demonstrated by the resulted negative values of ΔG_{ads}° . Typically, an
 384 endothermic adsorption process that has a positive value of ΔH_{ads}° is attributed unequivocally to
 385 chemisorption, while an exothermic adsorption process with ΔH_{ads}° of negative value may
 386 involve either physisorption or chemisorption, or a combination of both the processes [22]. In
 387 this study, the ΔH_{ads}° was positive, once again implying a chemisorption mechanism. The value
 388 of ΔS_{ads}° decreased with increased temperature, implying that the reaction of adsorption was

389 getting less disordered.

390 FTIR

391 The trend in the IR spectrum of the synthetic EPS followed closely to the natural WAS
392 EPS [8] as expected because it is formulated based on the chemical composition of natural WAS
393 EPS. Similar to the natural WAS EPS, the FTIR results of synthetic EPS showed that functional
394 groups O-H, N-H, C-N, C=O, and C-H were present. Since the synthetic EPS and natural WAS
395 EPS both have the same functional group, it can be deduced that these functional groups play
396 major roles in corrosion inhibition. Other authors have also suggested the contribution of these
397 functional groups in corrosion inhibition [28][29].

398 The electrochemical theory of corrosion holds that the metal surface corroding in an
399 electrolyte is covered with local electrolytic cells. Some areas of the metal can act as anodes and
400 other areas can act as cathodes, shown in Figure 10, depending upon the history of the metal
401 regarding heat treatment, presence of imperfections, scratches, greases, paint coatings,
402 fingerprint smudges, etc. At anodic sites, the metal usually dissolves into solution. Electrons
403 given from these sites are transported to local cathodes and collected by electron acceptors such
404 as hydrogen ions and oxygen. As previously suggested, synthetic EPS acts as a mixed-type
405 corrosion inhibitor, meaning that the molecules in the synthetic EPS chemisorbed on both the
406 anodic and cathodic sites of metal surface to form a monolayer protection film. The functional
407 groups rich in nitrogen and oxygen atoms acted as the polar head of organic corrosion inhibitors,
408 adsorbing on metal surface by forming chemical bonds between the inhibitor molecules and
409 metal ions, while the non-polar hydrocarbon chain attached to the polar head isolated the metal
410 surface from the corrosive surrounding, suppressing both anodic and cathodic corrosion
411 reactions, reducing the overall corrosion rate.

412

413 Operation and economic significance of synthetic EPS

414 The corrosion inhibition performance of the synthetic EPS shown in this study is
415 promising. Other areas that are interesting to be investigated are the operational and economical
416 sides of this corrosion inhibitor formulation.

417 Similar to most bio-inspired materials, this corrosion inhibitor formulation can be
418 formulated with commercial renewable resources or extracted from natural resources (waste
419 activated sludge), leaving a lesser environmental impact compared to the commercial petroleum-
420 based corrosion inhibitors. Besides having corrosion inhibition performance comparable to
421 commercial products (commercial products usually show inhibition performance above 70%),
422 the synthetic EPS is also just as easy to be applied like commercial corrosion inhibitors, making
423 it an excellent alternative.

424 The economic analysis of synthetic EPS was evaluated in this study. The production cost
425 of the synthetic EPS is about \$4.23 for every 10,000-inhibition treatment (assuming 1 L
426 system/treatment), while the market price of a typical commercial oil and gas corrosion inhibitor
427 costs about \$2.38 per 10,000 applications. It is worth mentioned that the synthetic EPS is
428 formulated based solely on the composition of natural EPS. The economic feasibility can be

429 improved in future studies by product optimization to reduce the applied inhibitor concentration
430 and enhance the inhibition performance.

431 It is evident that bio-inspired systems/materials have high potential in revolutionizing the
432 current market to reduce dependence on fossil fuel-based products as well as to promote
433 innovative product development approach. This transformation is not only applicable in the
434 corrosion inhibitor industry but should also be extended to benefit other research and
435 development areas.

436

437 **Conclusions**

438 The studied inhibitor, synthetic EPS, is a surrogate of biomass-based corrosion inhibitor
439 inspired by sources with varied chemical compositions to overcome the composition
440 inconsistency in biomass that can cause unreliable corrosion inhibition performance. Synthetic
441 EPS is a mixture of glutamic acid, carboxymethylcellulose, humic acid, thymine, and alginic
442 acid, following the chemical composition of natural WAS EPS extracted by heating method.
443 Unlike the natural WAS EPS that is rich in assorted of molecules that could promote stearic
444 hindrance on the adsorption of inhibitor molecules, synthetic EPS was designed specifically
445 based on the EPS groups that are known to perform as corrosion inhibitors. With concentration
446 of 204 mg/L in 3.64% NaCl saturated with CO₂ gas, synthetic EPS showed maximum corrosion
447 inhibitions of 82.41%, 89.65%, and 93.99% at 25°C, 50°C, and 70°C, respectively. Its
448 performance compared favorably with natural WAS EPS and commercial corrosion inhibitors.

449 The adsorption mechanism adhered to Langmuir isotherm, implying monolayer
450 adsorption. It was found that the inhibition performance was controlled by both the concentration
451 of inhibitor and temperature.

452 The corrosion inhibition capability was due to chemisorption shown by several
453 evidences:

- 454 (1) An increase in corrosion inhibition efficiency with increase temperature
- 455 (2) A decrease in activation energy in the presence of inhibitor
- 456 (3) The adsorption isotherm conforms to the Langmuir monolayer mechanism
- 457 (4) Endothermic adsorption

458 Since the formulation of synthetic EPS was designed solely based on the chemical
459 composition of natural WAS EPS, it was not optimized to meet the purpose of corrosion
460 inhibition. Based on the results presented and the needs and requirements of corrosion protection
461 service providers, the future direction of the current research will focus on optimizing the
462 formulation in order to reduce the required applied concentration of corrosion inhibitor while
463 achieving the maximum attainable corrosion inhibition performance. This could be done by first
464 reducing the number of compounds in the formulation, then optimizing the concentration of the
465 compounds and the inhibition performance statistically.

466 This bio-inspired material is developed in the hope to promote the commercialization of
467 renewable corrosion inhibitors. According to the Google Scholar database, there are as many as

468 17,600 publications on the topic of green corrosion inhibitors from the year 1980 to 2018. A
469 significant portion of these publications were made up by phytochemical-based compounds.
470 Plant extracts are gaining popularity as green corrosion inhibitors candidates not only because
471 they are renewable sources, but also their potential in corrosion mitigation. On average, the
472 attainable corrosion protection efficiencies of these inhibitors can range from 70% to as high as
473 98% [30][31][32][33][34]. Despite the overwhelming research evidence that suggests the
474 impressive performance of these inhibitors, there are still drastic uneven numbers of research
475 reports and products on the shelves. Needless to say, resource recovery efforts take time to
476 improve. Before these techniques are optimized, or if there are enough products to be added to
477 the product line to improve the cost issue [35], until then, bio-inspired material could be an
478 alternative to balance the environmental problems bring by petroleum-based corrosion inhibitors
479 and the economic complications raise by plant extracts corrosion inhibitors. As a matter of
480 course, the idea of benefiting from bio-inspired systems and materials will not only benefit the
481 corrosion inhibitor sector but is prompt to be extended to any other applicable research area.

482 **References**

- 483 [1] H. Liu and H. H. P. Fang, "Extraction of extracellular polymeric substances (EPS) of
484 sludges," *J. Biotechnol.*, vol. 95, no. 3, pp. 249–256, 2002.
- 485 [2] P. Cescutti, R. Toffanin, P. Pollesello, and I. W. Sutherland, "Structural determination of
486 the acidic exopolysaccharide produced by a *Pseudomonas* sp. strain 1.15," *Carbohydr.*
487 *Res.*, vol. 315, no. 1, pp. 159–168, 1999.
- 488 [3] L. Kennedy and I. W. Sutherland, "Polysaccharide lyases from gellan-producing
489 *Sphingomonas* spp.," *Microbiology*, vol. 142, no. 4, pp. 867–872, Apr. 1996.
- 490 [4] M. C. Veiga, M. K. Jain, W. Wu, R. I. Hollingsworth, and J. G. Zeikus, "Composition and
491 role of extracellular polymers in methanogenic granules.," *Appl. Environ. Microbiol.*, vol.
492 63, no. 2, pp. 403–407, 1997.
- 493 [5] B. F. Nielsen, T. Griebe, and P. H. Nielsen, "Enzymatic activity in the activated-sludge
494 floc matrix," *Appl. Microbiol. Biotechnol.*, vol. 43, no. 4, pp. 755–761, 1995.
- 495 [6] H. Ji, "Polymerization of humic substances in natural environments," in *Humic substances*
496 *and their role in the environment*, Chichester: Wiley, 1988, pp. 45–58.
- 497 [7] B. Frølund, R. Palmgren, K. Keiding, and P. H. Nielsen, "Extraction of extracellular
498 polymers from activated sludge using a cation exchange resin," *Water Res.*, vol. 30, no. 8,
499 pp. 1749–1758, 1996.
- 500 [8] L. C. Go, W. Holmes, D. Depan, and R. Hernandez, "Evaluation of extracellular
501 polymeric substances extracted from waste activated sludge as a renewable corrosion
502 inhibitor," *PeerJ*, vol. 7, p. e7193, Jun. 2019.
- 503 [9] L. C. Go, W. Holmes, and R. Hernandez, "Sweet corrosion inhibition on carbon steel
504 using waste activated sludge extract," in *2019 IEEE Green Technologies*
505 *Conference(GreenTech)*, 2019, pp. 1–4.
- 506 [10] S. Comte, G. Guibaud, and M. Baudu, "Relations between extraction protocols for
507 activated sludge extracellular polymeric substances (EPS) and EPS complexation
508 properties: Part I. Comparison of the efficiency of eight EPS extraction methods," *Enzyme*
509 *Microb. Technol.*, vol. 38, no. 1, pp. 237–245, 2006.
- 510 [11] D. S. HOARE, "THE BREAKDOWN AND BIOSYNTHESIS OF GLUTAMIC ACID,"
511 *J. Gen. Microbiol.*, vol. 32, no. 2, pp. 157–161, Aug. 1963.
- 512 [12] D.-Q. Zhang, Q.-R. Cai, L.-X. Gao, and K. Y. Lee, "Effect of serine, threonine and
513 glutamic acid on the corrosion of copper in aerated hydrochloric acid solution," *Corros.*
514 *Sci.*, vol. 50, no. 12, pp. 3615–3621, 2008.
- 515 [13] D.-Q. Zhang, Q.-R. Cai, X.-M. He, L.-X. Gao, and G.-D. Zhou, "Inhibition effect of some
516 amino acids on copper corrosion in HCl solution," *Mater. Chem. Phys.*, vol. 112, no. 2,
517 pp. 353–358, 2008.
- 518 [14] M. M. Solomon, S. A. Umoren, I. I. Udosoro, and A. P. Udoh, "Inhibitive and adsorption
519 behaviour of carboxymethyl cellulose on mild steel corrosion in sulphuric acid solution,"
520 *Corros. Sci.*, vol. 52, no. 4, pp. 1317–1325, 2010.

- 521 [15] E. BAYOL, A. GURTEN, M. DURSUN, and K. KAYAKIRILMAZ, “Adsorption
522 Behavior and Inhibition Corrosion Effect of Sodium Carboxymethyl Cellulose on Mild
523 Steel in Acidic Medium,” *Acta Physico-Chimica Sin.*, vol. 24, no. 12, pp. 2236–2243,
524 Dec. 2008.
- 525 [16] M. S. Morad, “Inhibition of phosphoric acid corrosion of zinc by organic onium
526 compounds and their adsorption characteristics,” *J. Appl. Electrochem.*, vol. 29, pp. 619–
527 626, 1999.
- 528 [17] M. Abdallah, “Guar Gum as Corrosion Inhibitor for Carbon Steel in Sulfuric Acid
529 Solutions,” *Port. Electrochim. Acta*, vol. 22, pp. 161–175, 2004.
- 530 [18] M. Bouklah, B. Hammouti, M. Lagrenée, and F. Bentiss, “Thermodynamic properties of
531 2,5-bis(4-methoxyphenyl)-1,3,4-oxadiazole as a corrosion inhibitor for mild steel in
532 normal sulfuric acid medium,” *Corros. Sci.*, vol. 48, no. 9, pp. 2831–2842, 2006.
- 533 [19] Harish Kumar and Vikas Yadav, “Citrus sinensis peels as a Green Corrosion Inhibitor for
534 Mild Steel in 5.0 M Hydrochloric Acid Solution,” *Res. J. Chem. Sci.*, vol. 6, no. 1, pp. 53–
535 60, 2016.
- 536 [20] N. Chaubey, V. K. Singh, and M. A. Quraishi, “Effect of some peel extracts on the
537 corrosion behavior of aluminum alloy in alkaline medium,” *Int. J. Ind. Chem.*, vol. 6, no.
538 4, pp. 317–328, Nov. 2015.
- 539 [21] R. Myrdal, “Corrosion Inhibitors– State of the art,” 2010.
- 540 [22] F. Bentiss, M. Lebrini, and M. Lagrenée, “Thermodynamic characterization of metal
541 dissolution and inhibitor adsorption processes in mild steel/2,5-bis(n-thienyl)-1,3,4-
542 thiadiazoles/hydrochloric acid system,” *Corros. Sci.*, vol. 47, no. 12, pp. 2915–2931,
543 2005.
- 544 [23] A. Popova, E. Sokolova, S. Raicheva, and M. Christov, “AC and DC study of the
545 temperature effect on mild steel corrosion in acid media in the presence of benzimidazole
546 derivatives,” *Corros. Sci.*, vol. 45, no. 1, pp. 33–58, 2003.
- 547 [24] F. S. de Souza and A. Spinelli, “Caffeic acid as a green corrosion inhibitor for mild steel,”
548 *Corros. Sci.*, vol. 51, no. 3, pp. 642–649, Mar. 2009.
- 549 [25] A. Al-Amiery, A. Kadhum, A. Kadhum, A. Mohamad, C. How, and S. Junaedi,
550 “Inhibition of Mild Steel Corrosion in Sulfuric Acid Solution by New Schiff Base,”
551 *Materials (Basel)*, vol. 7, no. 2, pp. 787–804, Jan. 2014.
- 552 [26] E. Khamis, “The Effect of Temperature on the Acidic Dissolution of Steel in the Presence
553 of Inhibitors,” *Corrosion*, vol. 46, no. 6, pp. 476–484, 1990.
- 554 [27] “Thermodynamics and Kinetics of Adsorption.” [Online]. Available: http://w0.rz-berlin.mpg.de/imprs-cs/download/Vortrag_IMPRS_Schmoeckwitz_Mi_9-11_KChrist.pdf.
555
- 556 [28] E. E. Ebenso, N. O. Eddy, and A. O. Odiongenyi, “Corrosion inhibitive properties and
557 adsorption behaviour of ethanol extract of Piper guinensis as a green corrosion inhibitor
558 for mild steel in H₂SO₄,” *African J. Pure Appl. Chem.*, vol. 2, no. 11, pp. 107–115, 2008.

- 559 [29] E. I. Ating, S. A. Umoren, I. I. Udousoro, E. E. Ebenso, and A. P. Udoh, "Leaves extract
560 of *Ananas sativum* as green corrosion inhibitor for aluminium in hydrochloric acid
561 solutions," *Green Chem. Lett. Rev.*, vol. 3, no. 2, pp. 61–68, Jun. 2010.
- 562 [30] N. O. Eddy and E. E. Ebenso, "Adsorption and inhibitive properties of ethanol extracts of
563 *Musa sapientum* peels as a green corrosion inhibitor for mild steel in H₂SO₄," *African J.*
564 *Pure Appl. Chem.*, vol. 2, no. 6, pp. 46–54, 2008.
- 565 [31] Taleb H. Ibrahim, Youssef Chehade, and Mohamed Abou Zour, "Corrosion Inhibition of
566 Mild Steel using Potato Peel Extract in 2M HCl Solution," *Int. J. Electrochem. Sci.*, vol. 6,
567 pp. 6542–6556, 2011.
- 568 [32] H. Elmsellem, H. Bendaha, A. Aouniti, A. Chetouani, M. Mimouni, and A. Bouyanzer,
569 "Comparative study of the inhibition of extracts from the peel and seeds of *Citrus*
570 *Aurantium* against the corrosion of steel in molar HCl solution," *Moroccan J. Chem.*, vol.
571 2, no. 1, pp. 1–9, 2014.
- 572 [33] Janaina Cardozo da Rocha, José Antônio da Cunha Ponciano Gomes, and Eliane D'Elia,
573 "Aqueous extracts of mango and orange peel as green inhibitors for carbon steel in
574 hydrochloric acid solution," *Mater. Res.*, vol. 17, no. 6, pp. 1516–1439, 2014.
- 575 [34] M. Sangeetha, S. Rajendran, J. Sathiyabama, and P. Prabhakar, "Eco friendly extract of
576 Banana peel as corrosion inhibitor for carbon steel in sea water," *J. Nat. Prod. Plant*
577 *Resour.*, vol. 2, no. 5, pp. 601–610, 2012.
- 578 [35] L. C. Go *et al.*, "Biobased chemical and energy recovered from waste microbial matrices,"
579 *Curr. Opin. Chem. Eng.*, vol. 26, pp. 65–71, Dec. 2019.

580

581

582

Table 1 (on next page)

Details of synthetic EPS

Type	Chemical	Vendor	Specification	Amount (mg/L)
Protein	Glutamic acid	Acros Organics	99%	30
Carbohydrate	Carboxymethyl cellulose (CMC)	Acros Organics	MW 70,000	12
Humic acid	Humic acid	Acros Organics	45-70%	5
Nucleic acid	Thymine	Alfa Aesar	97%	2
Uronic acid	Alginic acid, sodium salt	Acros Organics	-	2

1

Table 2 (on next page)

Electrochemical parameters and the corresponding corrosion inhibition efficiencies in the presence of different concentrations of synthetic EPS at various temperatures

Temperature (°C)	Temperature (K)	Concentration (mg/L)	E_{corr} (V)	I_{corr} ($\mu\text{A}/\text{cm}^2$)	Inhibition efficiency (%)	Surface coverage degree, θ
25	298	0	-0.73	52.48	-	-
		51	-0.71	25.12	68.72	0.6872
		102	-0.71	18.20	77.34	0.7734
		153	-0.71	14.45	82.00	0.8200
		204	-0.70	14.13	82.41	0.8241
50	323	0	-0.74	125.89	-	-
		51	-0.76	37.15	86.03	0.8603
		102	-0.76	34.67	86.96	0.8696
		153	-0.76	33.11	87.55	0.8755
		204	-0.76	27.54	89.65	0.8965
70	343	0	-0.73	223.87	-	-
		51	0.76	45.71	91.70	0.9170
		102	-0.76	39.81	92.77	0.9277
		153	-0.76	34.67	93.71	0.9371
		204	0.75	33.11	93.99	0.9399

1

Table 3 (on next page)

Corrosion kinetic parameters for carbon steel in different concentrations of the synthetic EPS

Inhibitor concentration (mg/L)	E _a (kJ/mol)	ΔH _a ^o (kJ/mol)	ΔS _a ^o (J/mol K)
0	27.46	24.81	-71.28
51	12.54	8.75	-131.24
102	15.21	12.56	-120.83
153	17.24	14.59	-115.63
204	16.47	13.82	-118.73

1

Table 4(on next page)

Thermodynamic parameters for the adsorption of synthetic EPS at different temperatures

Temperature (°C)	Temperature (K)	R ²	K ([mg/L] ⁻¹)	$\Delta G_{\text{ads}}^{\circ}$ (kJ/mol)	$\Delta H_{\text{ads}}^{\circ}$ (kJ/mol)	$\Delta S_{\text{ads}}^{\circ}$ (J/mol K)
25	298	0.9980	0.01039	-22.93	7.5192	102.11
50	323	0.9969	0.01325	-23.53		72.81
70	343	0.9999	0.01545	-23.91		69.68

1

Table 5 (on next page)

Characteristic IR absorption frequencies of organic functional groups

Characteristic Absorptions (cm ⁻¹)	Vibration Type	Functional Type
3,200 - 3,600	Phenol OH stretch	OH into polymeric compounds
2,850 - 3,000	Alkane C-H stretch	
1,690 - 1,630	Amide C=O stretch	Proteins
1,590 - 1,650	Amide (I) N-H bend	
1,500 - 1,560	Amide (II) N-H bend	
1,350 - 1,480	Alkane C-H bending	
1,080 - 1,360	Amine C-N stretch	

1

Figure 1

Tafel plot for carbon steel in 3.64% NaCl concentrated with CO₂ with different concentrations of synthetic EPS at 25°C

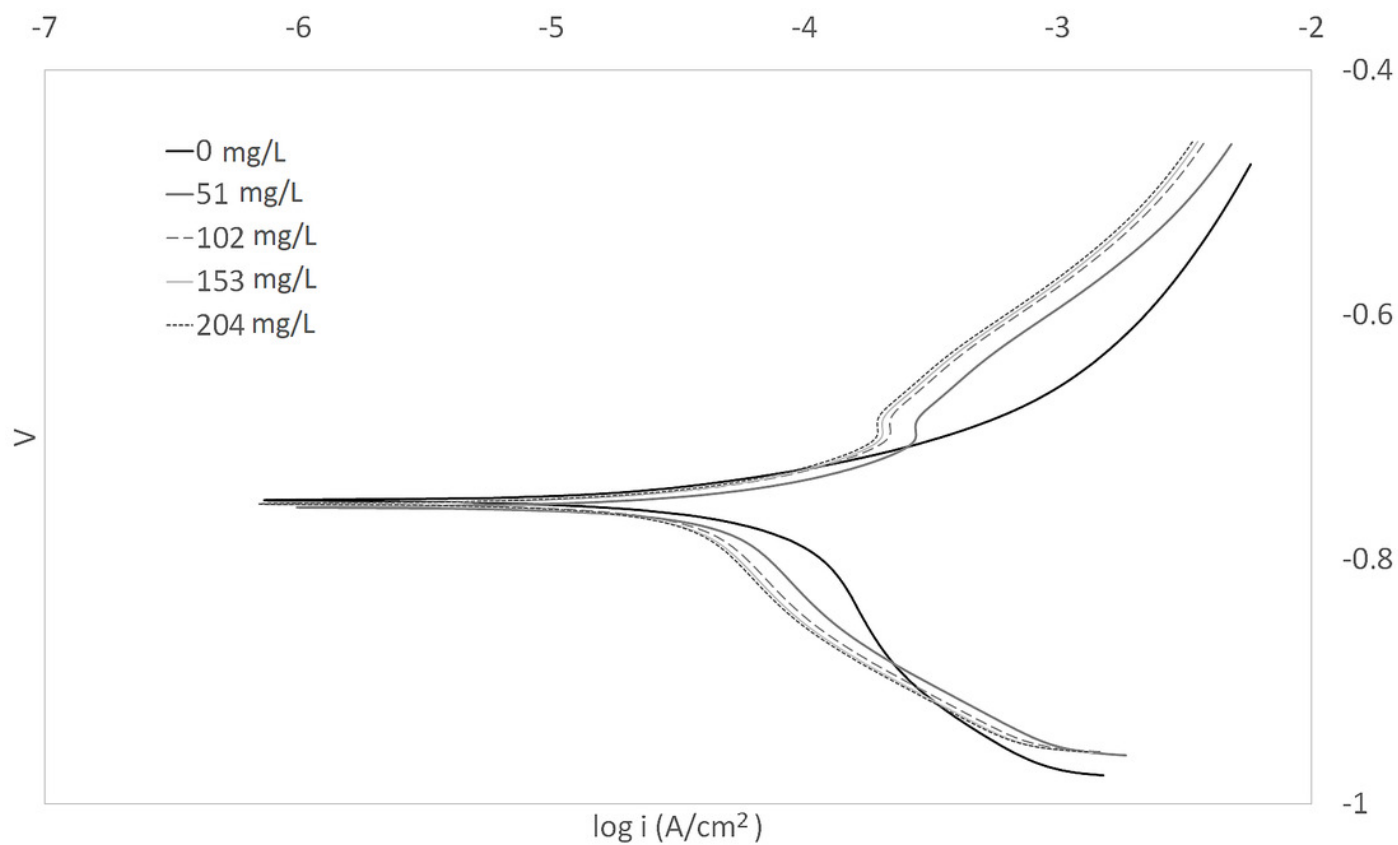


Figure 2

Tafel plot for carbon steel in 3.64% NaCl concentrated with CO₂ with different concentrations of synthetic EPS at 50°C

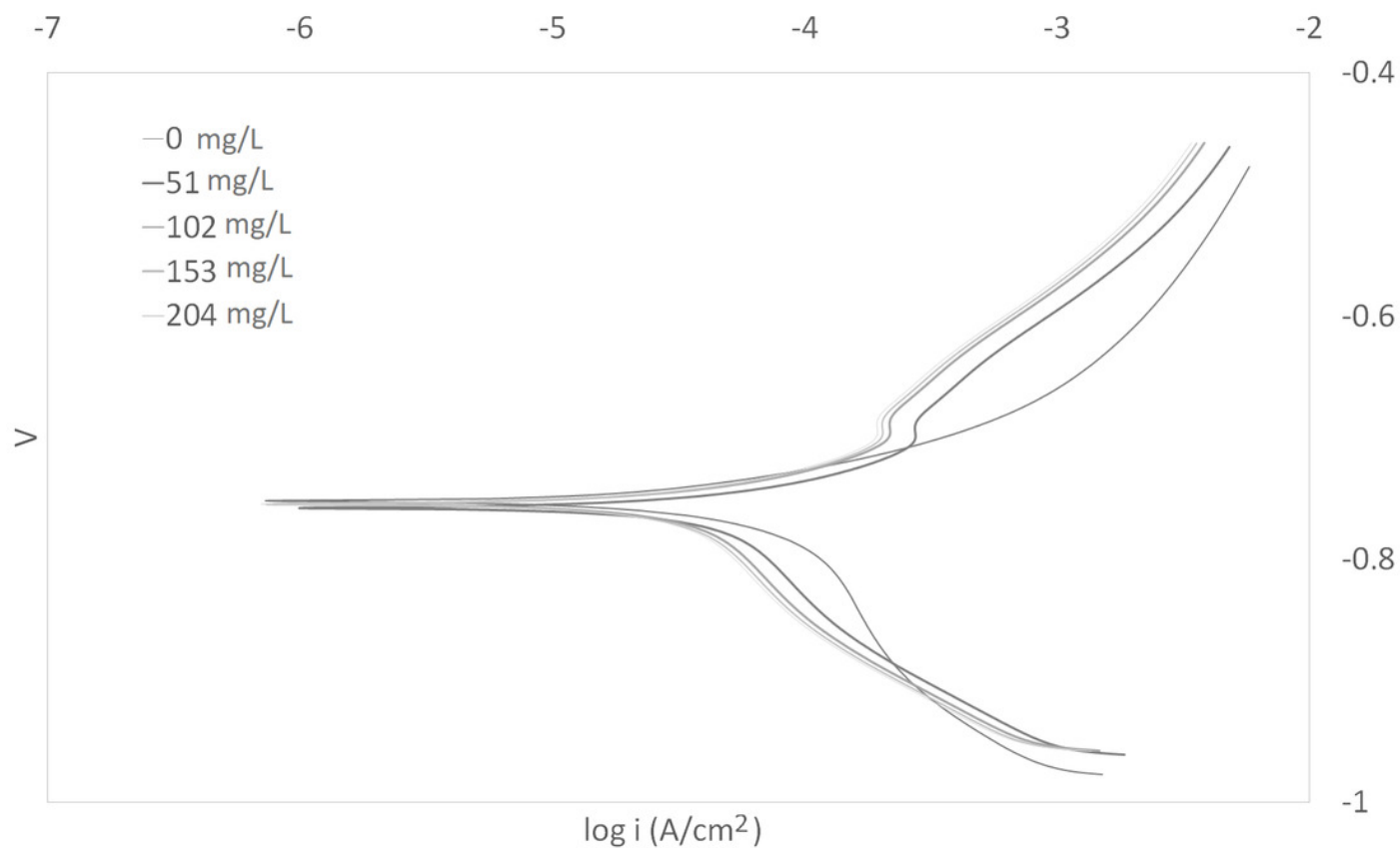


Figure 3

Tafel plot for carbon steel in 3.64% NaCl concentrated with CO₂ with different concentrations of synthetic EPS at 70°C

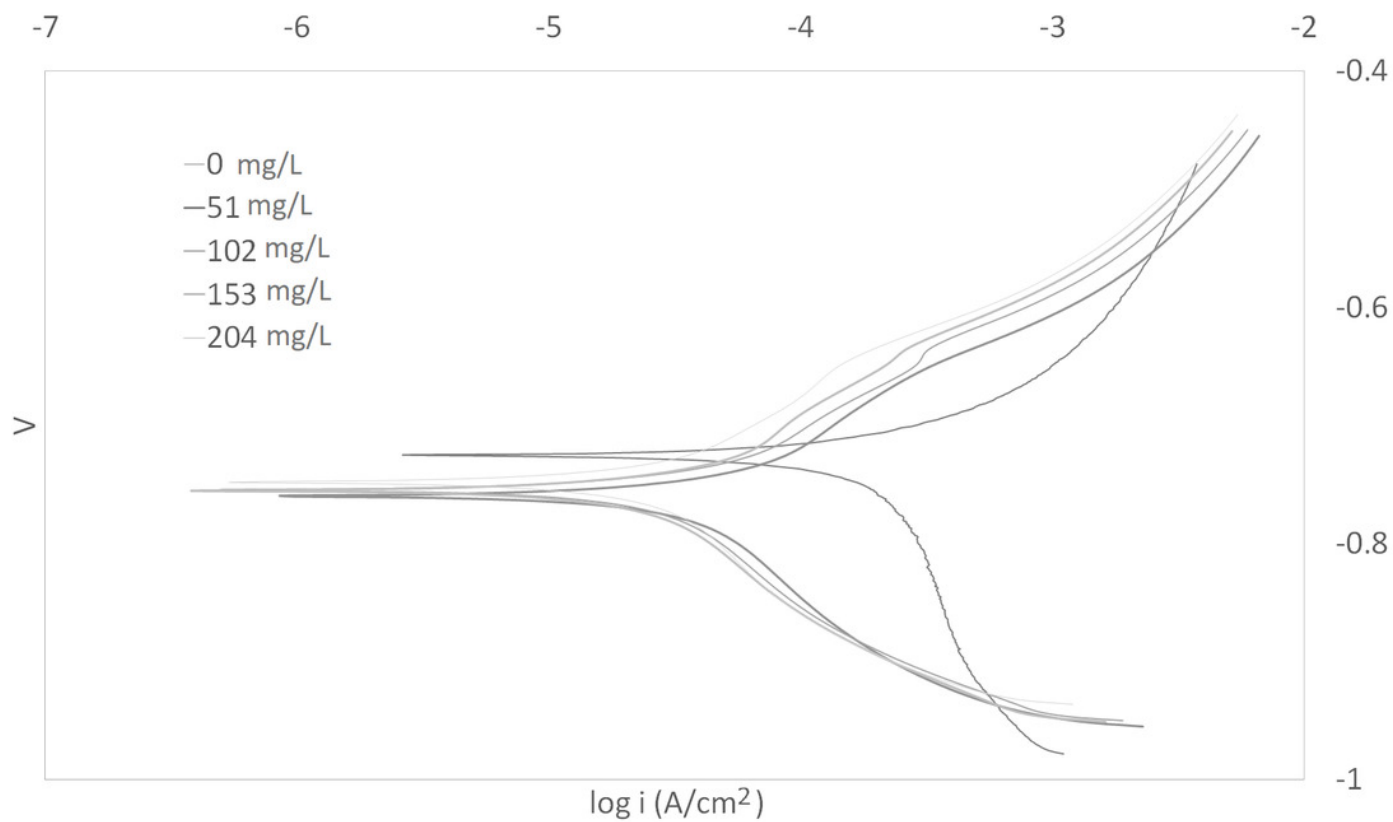


Figure 4

Arrhenius plots of $\ln I_{\text{corr}}$ versus $1/T$ at different concentrations of synthetic EPS

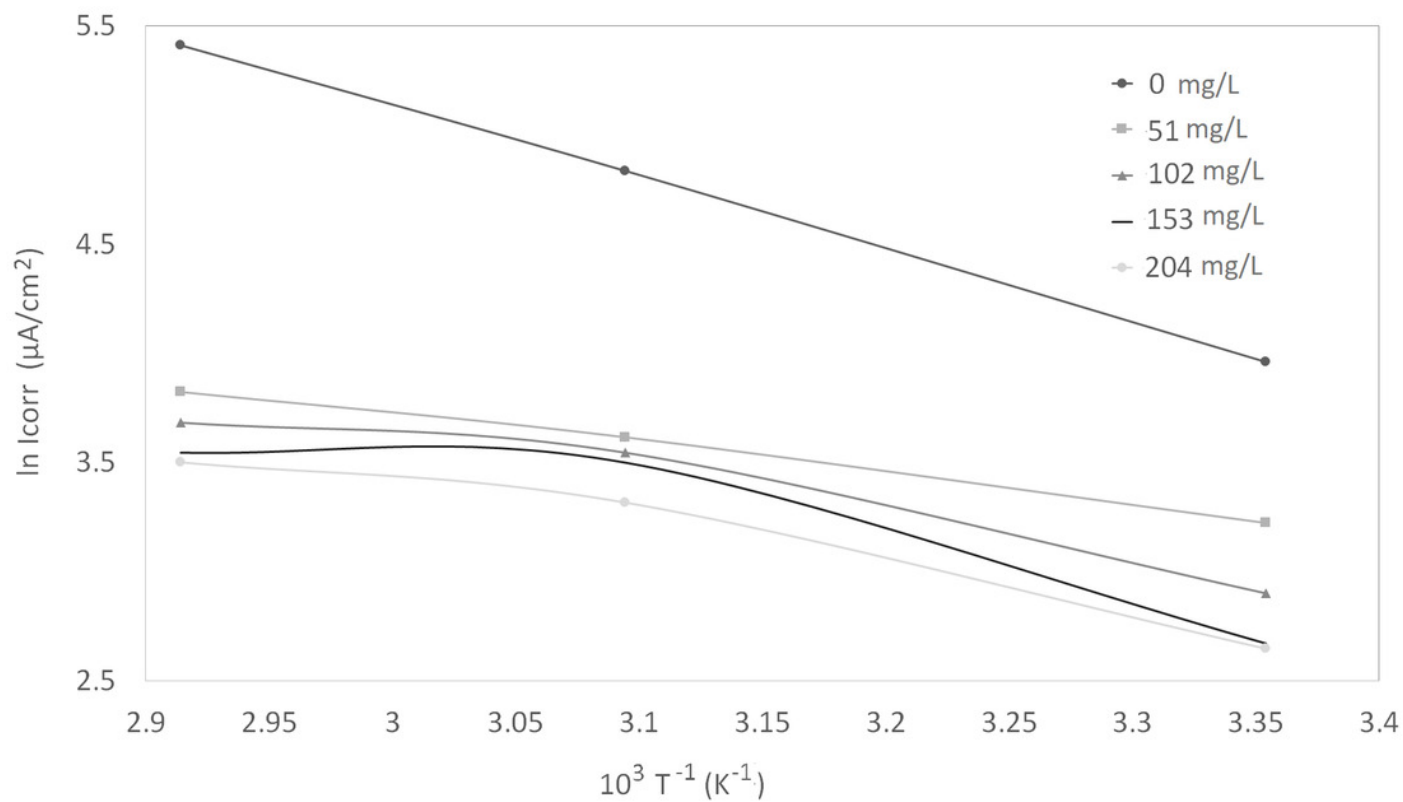


Figure 5

Arrhenius plots of corrosion $\ln(I_{\text{corr}}/T)$ versus $1/T$ at different concentrations of synthetic EPS

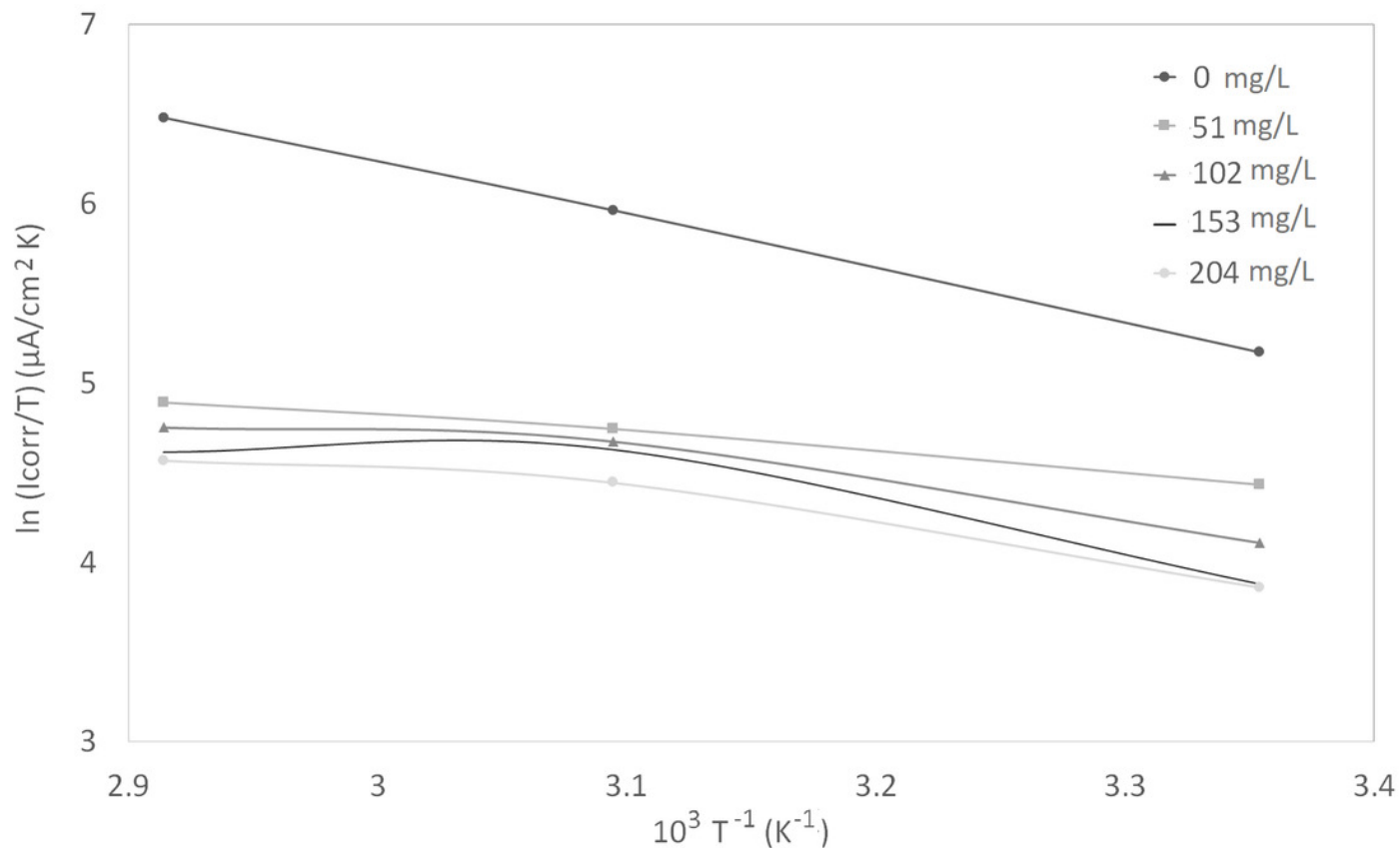


Figure 6

Curve fitting of the experimental data to Langmuir isotherm

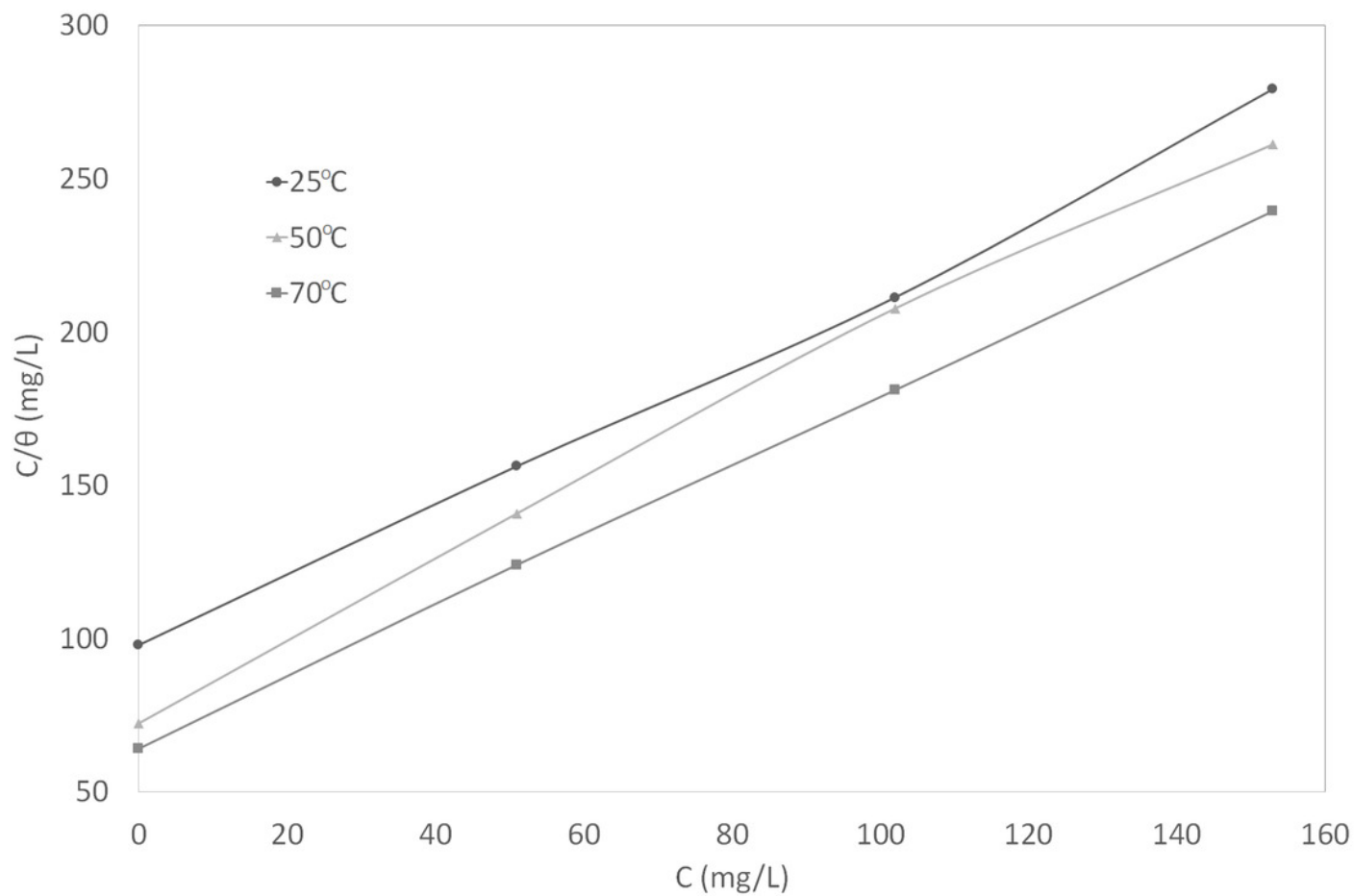


Figure 7

Van't Hoff plot

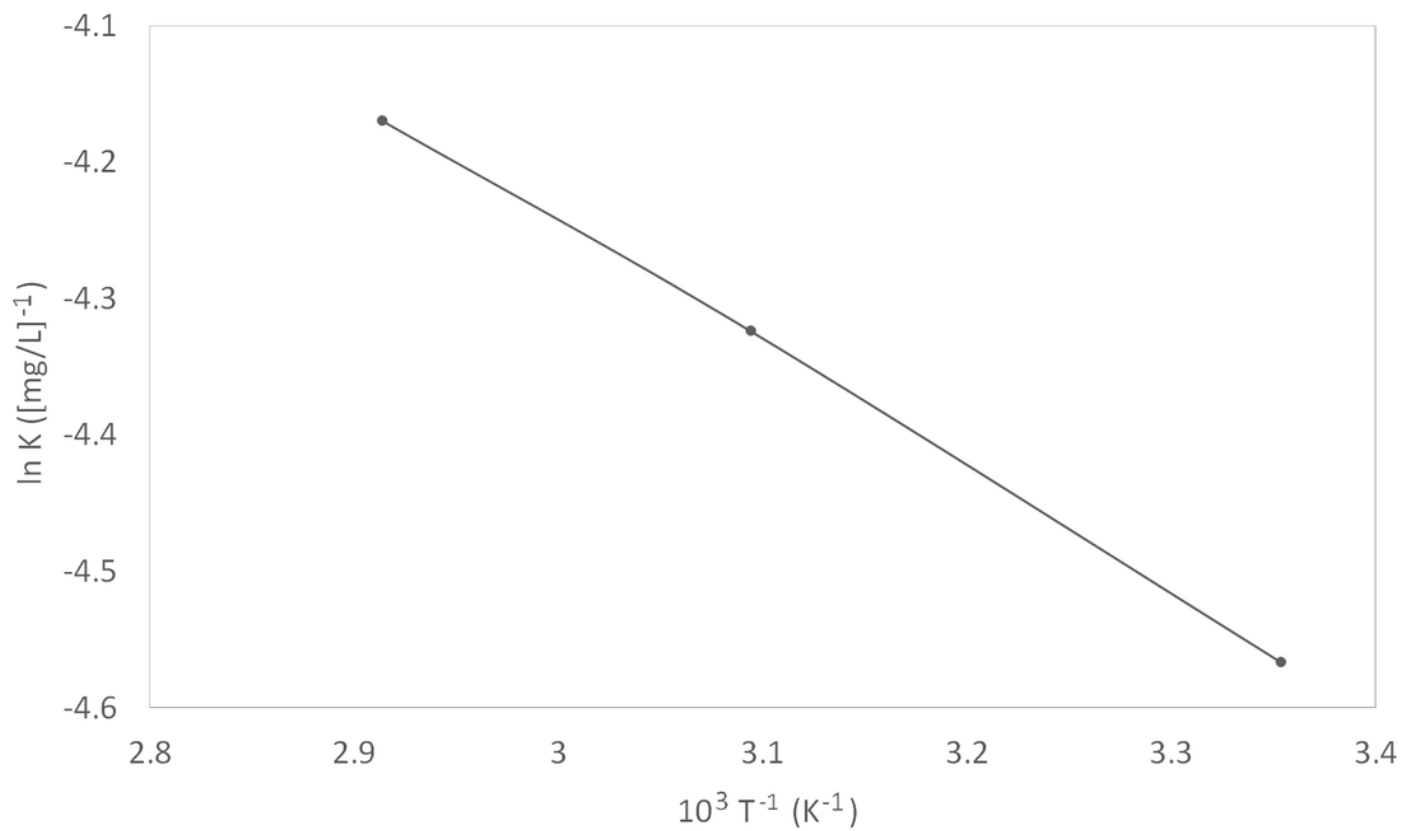


Figure 8

IR spectra of synthetic EPS

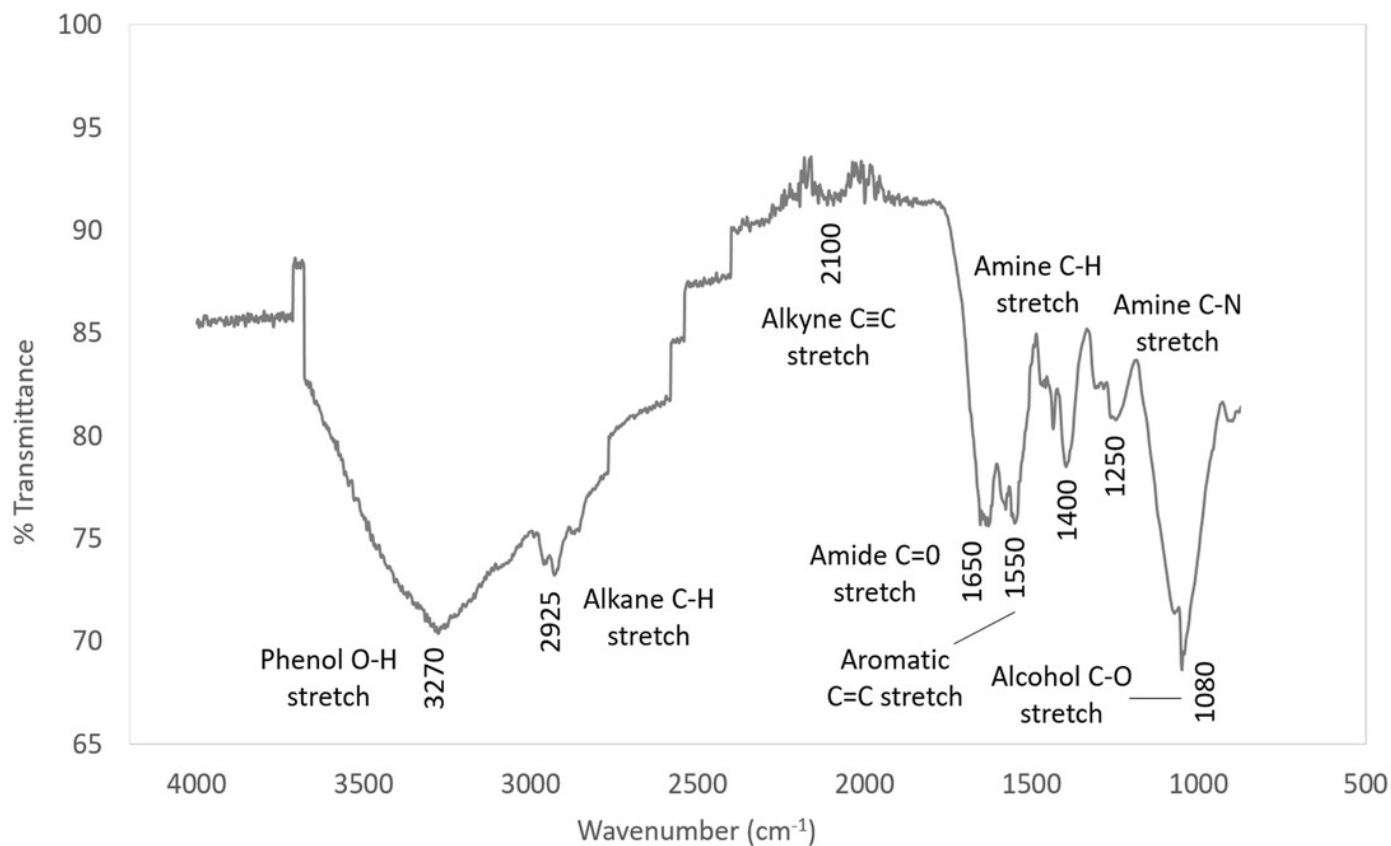


Figure 9

Chemicals in synthetic EPS and their structures

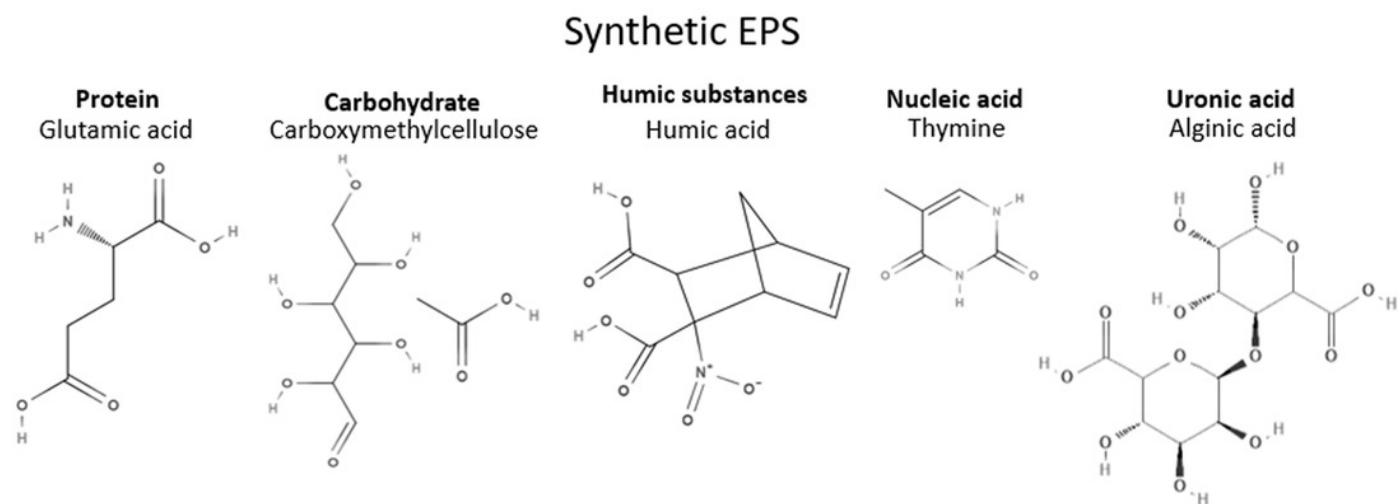


Figure 10

Corrosion inhibition mechanism of synthetic EPS

I: Inhibitor

